Astron. Astrophys. 361, 937–944 (2000)

ASTRONOMY AND ASTROPHYSICS

Blue horizontal branch stars in metal-rich globular clusters

II. 47 Tucanae and NGC 362

S. Moehler[1,⋆], **W.B. Landsman**[2], **and B. Dorman**[2]

[1] Dr. Remeis-Sternwarte, Astronomisches Institut der Universität Erlangen-Nürnberg, Sternwartstrasse 7, 96049 Bamberg, Germany (ai13@sternwarte.uni-erlangen.de)
[2] Raytheon ITSS, NASA/GSFC, Greenbelt, MD 20770, USA (landsman@mpb.gsfc.nasa.gov; dorman@veris.gsfc.nasa.gov)

Received 3 July 2000 / Accepted 11 August 2000

Abstract. Atmospheric parameters ($T_{\rm eff}$, $\log g$), and radial velocities are derived for twelve candidate blue horizontal branch (HB) stars in the globular clusters 47 Tuc and NGC 362, which so far have been known to contain primarily red HB stars. The spectroscopic targets were selected from the catalog of hot stars detected in these clusters at 1600 Å using the Ultraviolet Imaging Telescope (UIT). Spectroscopic analyses of these stars reveal, however, that one of the four HB candidates targets in 47 Tuc, and five out of the eight targets in NGC 362 are probably background stars belonging to the Small Magellanic Cloud. With the exception of the photometric binary *MJ38529* in 47 Tuc, the parameters of those stars that are probable members of 47 Tuc and NGC 362 agree well with canonical HB evolution. The three hot stars in 47 Tuc all have $10{,}000\,{\rm K} < T_{\rm eff} < 15{,}000\,{\rm K}$ and include one photometric binary, which suggests that they might have a different physical origin than the dominant red HB population. The somewhat cooler blue HB stars in NGC 362 show more continuity with the dominant red HB population and might simply arise from red giants with unusually high mass loss.

Key words: stars: early-type – stars: horizontal-branch – stars: Population II – Galaxy: globular clusters: individual: NGC 104, NGC 362

1. Introduction

The colour-magnitude diagrams (CMD's) of globular clusters show a great variety of horizontal branch (HB) morphologies. It has long been known that the HB morphology tends to become bluer with decreasing cluster metallicity. However, the existence of pairs of globular clusters with the same metallicity but different HB morphologies shows that there must be at least one "second parameter". Theoretically, an increase in age is expected to reduce the envelope mass and thus yield a bluer HB morphology, *provided that no other parameters are changing.* If age *is* the second parameter, then there are profound consequences for models of the formation of the galactic halo (e.g. Sarajedini et al. 1995) and the origin of the ultraviolet upturn in elliptical galaxies (e.g. Park & Lee 1997). However, much recent work indicates that age may not be the only or even the dominant second parameter controlling the HB morphology (Stetson et al. 1996, Ferraro et al. 1997a, Catelan 2000). Fusi Pecci et al. (1993) suggested that the cluster density may influence the extension of the blue HB to rather faint magnitudes ("blue tail") that is seen in the CMD's of many globular clusters, due to enhanced mass loss triggered by stellar interactions (see also Bailyn 1995).

The clusters 47 Tuc and NGC 362 are famous for their red HB morphologies. 47 Tuc is the prototype metal-rich ([Fe/H] = −0.71; Harris 1996) red HB cluster, with only a single known RR Lyr star (V9; Carney et al. 1993). NGC 362 ([Fe/H] = −1.16; Harris 1996) is the red member of a famous second-parameter pair of clusters (along with NGC 288). Thus it was a surprise when observations with the Ultraviolet Imaging Telescope (UIT) revealed the presence of 51 hot ($T_{\rm eff} > 8500$ K) stars in the field of 47 Tuc (O'Connell et al. 1997) and 84 hot stars within a radius of 8.′25 from the center of NGC 362 (Dorman et al. 1997). Although both 47 Tuc and NGC 362 are located in projection on the outer halo of the Small Magellanic Cloud (SMC), O'Connell et al. and Dorman et al. were able to show from the distribution with cluster radius that a significant fraction of the detected hot stars should be cluster members. Independently, Kaluzny et al. (1997, 1998a) used optical photometry to identify eight candidate blue HB stars in 47 Tuc (all of which were detected with UIT), but suggested from the absence of a radial gradient that most of these candidates were actually SMC halo members.

If the hot stars in NGC 362 and 47 Tuc are HB stars and cluster members, then they should have the same age and metallicity as the majority red HB population, and might provide important clues to the other parameters that can yield blue HB stars in globular clusters. However, as noted above, not all the hot stars detected on the UIT images are cluster HB stars. From the distribution of young stars in the outer halo of the SMC mapped by Gardiner & Hatzidimitriou (1992), we expect significant SMC

Send offprint requests to: S. Moehler

⋆ Based on observations collected at the European Southern Observatory (ESO N° 60.E-0145)

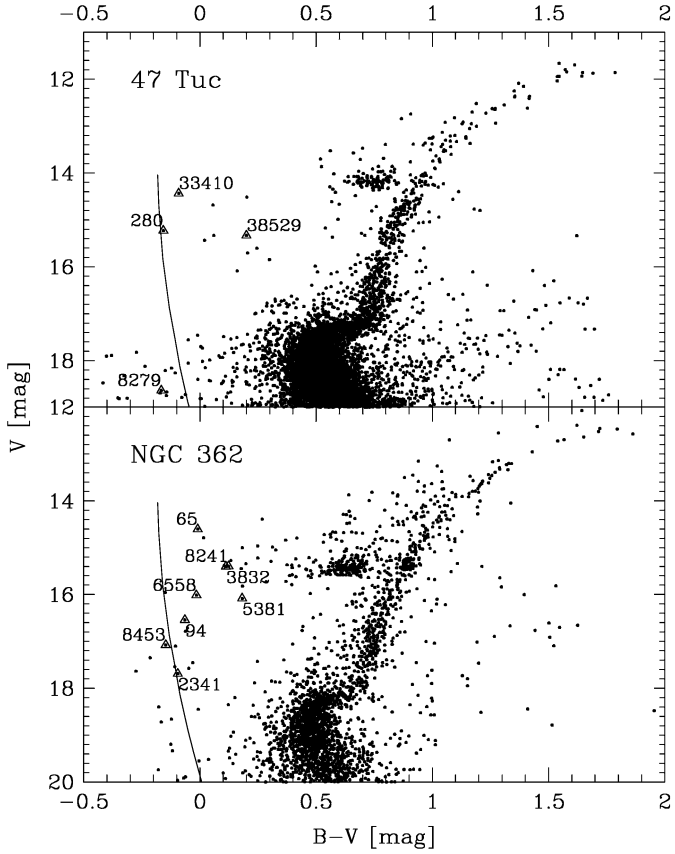

Fig. 1. The colour-magnitude diagrams for 47 Tuc and NGC 362 as observed by Montgomery & Janes (priv. comm.). The triangles mark the stars for which we took spectra (with the numbers referring to Table 1). The solid line marks the main sequence of the Small Magellanic Cloud, as derived from the interior models of Charbonnel et al. (1993) using the colour transformation of Kurucz (1992) and $(m - M)_0$ = $18\overset{\mathrm{m}}{.}91$ and $\mathrm{E_{B-V}} = 0\overset{\mathrm{m}}{.}09$ for the SMC.

contamination of the hot stars in NGC 362, whereas 47 Tuc is located in a region mostly devoid of young stars in the northwest SMC halo. Some of the hot stars in NGC 362 and 47 Tuc might also be extreme blue stragglers, analogous to those seen in the cores of NGC 6397 (Burgarella et al. 1994) and M3 (Ferraro et al. 1997b). The temperatures of these blue stragglers can reach 12,000 K, and recent HST spectroscopy has confirmed that the mass of the two bright blue stragglers in the core of NGC 6397 exceeds twice the turnoff mass (Sepinsky et al. 2000).

To reach any conclusions about these stars and their evolutionary status we need information about their atmospheric parameters (effective temperature and surface gravity) and also about their cluster membership. We therefore started a programme to obtain spectra of the hot HB star candidates in 47 Tuc and NGC 362. The radial velocities can be used to assess cluster membership, and the derived atmospheric parameters ($\mathrm{T_{eff}}$ and $\log \mathrm{g}$) can be used to distinguish HB stars from blue stragglers and background stars.

We describe the observations and their reduction Sects. 2 and 3. The determination of atmospheric parameters is described in Sect. 4 and the results are discussed in Sect. 5.

2. Observations

We selected a total of 12 blue stars in 47 Tuc and NGC 362 that were sufficiently uncrowded to allow ground-based follow-up spectroscopy. These stars are listed in Table 1 and marked in Fig. 1 with triangles.

We observed with the *ESO Multi Mode Instrument* (EMMI) at the *New Technology Telescope* (NTT) on October 26 and 27, 1997, using only the blue channel as the use of the two-channel mode leads to destructive interference around the H_β line. We obtained low resolution spectrophotometric data with large slit widths to analyse the flux distribution and medium resolution spectra to measure Balmer line profiles and helium line equivalent widths. Seeing values for these observations varied between $0\overset{''}{.}7$ and $1\overset{''}{.}3$, but the nights were not photometric. Since no EMMI grism allows observations below 3600 Å (necessary to measure the Balmer jump) we used grating #4 (72 Å/mm) and reduced the dispersion for the low resolution spectra by binning along the dispersion axis by a factor of 4. We used a slit width of $1\overset{''}{.}0$ ($5\overset{''}{.}0$) for the medium (low) resolution spectra and the slit was kept at parallactic angle for all observations. The CCD was a Tek 1024×1024 chip with $(24\,\mu\mathrm{m})^2$ pixels, a read-out-noise of $5.7\mathrm{e}^-$ and a gain of $2.84\ \mathrm{e}^-$/count.

For calibration purposes we observed each night 10 bias frames and 10 dome flat-fields with a mean exposure level of about 10,000 counts each. In addition we obtained sky flat fields to correct for the slit illumination. We took wavelength calibration spectra before and after each science spectrum. As flux standard stars we used LTT 7987 and EG 21.

3. Data reduction

We averaged the bias frames of the two nights and used their mean value instead of the whole frames as there was no spatial or temporal variation detectable. To correct the electronic offset we adjusted the mean bias by the difference between the mean overscan value of the science frame and that of the bias frame. The dark currents were determined from several long dark frames and turned out to be negligible (3 ± 2 counts/hr/pixel).

The flat fields were averaged separately for each night, since there was a slight variation in the fringe patterns of the flat fields from one night to the next (below 5%). We averaged the sky flat fields and then condensed them along the dispersion axis to derive the spatial profile of the slit. The dome flat fields were treated the same way, divided by their spatial profile and then multiplied by the spatial profile derived from the sky flat fields. The spectral energy distribution of the flat field lamp was determined by averaging the dome flat fields along the spatial axis. This one-dimensional "flat field spectrum" was then heavily smoothed and was afterwards used to normalize the dome flats along the dispersion axis.

For the wavelength calibration we fitted 3^{rd} order polynomials to the dispersion relations. We rebinned the frames two-dimensionally to constant wavelength steps. Before the sky fit the frames were median filtered along the spatial axis to erase cosmic ray hits in the background. To determine the sky background we had to find regions without any stellar spectra, which

Table 1. Coordinates, photometric data, distance from cluster center, heliocentric radial velocities (obtained from our spectra), and cluster membership information (from proper motions) for the target stars in 47 Tuc and NGC 362. The numbers and the $B, B-V$ photometric data are from Montgomery & Janes (priv. comm.). m_{162} is the UIT magnitude at 1620 Å. The proper motion cluster membership is taken from Tucholke (1992a, 1992b).

Star	α_{2000}	δ_{2000}	B	$B-V$	m_{162}	$m_{162}-V$	dis [′]	$v_{rad,hel}$ [km s^{-1}]	proper motion member (probability)
				47 Tuc					
MJ280	$00^h21^m29\overset{s}{.}35$	$-71°58'14\overset{''}{.}3$	$15\overset{m}{.}07$	$-0\overset{m}{.}16$	$13\overset{m}{.}18$	$-2\overset{m}{.}05$	5.6	-37	96.8% (T1948)
MJ8279	$00^h22^m57\overset{s}{.}71$	$-71°57'56\overset{''}{.}6$	$18\overset{m}{.}47$	$-0\overset{m}{.}17$	$15\overset{m}{.}86$	$-2\overset{m}{.}78$	13.7	$+161$	—
MJ33410	$00^h24^m44\overset{s}{.}79$	$-72°09'33\overset{''}{.}1$	$14\overset{m}{.}34$	$-0\overset{m}{.}09$	$13\overset{m}{.}70$	$-0\overset{m}{.}73$	9.0	-25	—
MJ38529	$00^h25^m33\overset{s}{.}20$	$-72°10'44\overset{''}{.}3$	$15\overset{m}{.}54$	$+0\overset{m}{.}20$	$13\overset{m}{.}82$	$-1\overset{m}{.}51$	8.6	-46	97.8% (T300)
				NGC 362					
MJ65	$01^h01^m58\overset{s}{.}4$	$-70°50'28\overset{''}{.}9$	$14\overset{m}{.}59$	$-0\overset{m}{.}01$	$14\overset{m}{.}97$	$+0\overset{m}{.}37$	6.2	$+120$	18.3% (T15)
MJ94	$01^h03^m18\overset{s}{.}7$	$-70°52'20\overset{''}{.}9$	$16\overset{m}{.}47$	$-0\overset{m}{.}07$	$15\overset{m}{.}04$	$-1\overset{m}{.}50$	6.1	$+137$	0.0% (T16)
MJ2341	$01^h03^m11\overset{s}{.}8$	$-70°51'20\overset{''}{.}8$	$17\overset{m}{.}59$	$-0\overset{m}{.}10$	$15\overset{m}{.}29$	$-2\overset{m}{.}40$	3.9	$+75$	—
MJ3832	$01^h03^m04\overset{s}{.}5$	$-70°51'30\overset{''}{.}5$	$15\overset{m}{.}51$	$+0\overset{m}{.}11$	$15\overset{m}{.}19$	$-0\overset{m}{.}21$	1.0	$+197$	—
MJ5381	$01^h04^m17\overset{s}{.}8$	$-70°54'23\overset{''}{.}8$	$16\overset{m}{.}26$	$+0\overset{m}{.}18$	$16\overset{m}{.}38$	$+0\overset{m}{.}30$	5.5	$+109$	0.2% (T247)
MJ6558	$01^h03^m16\overset{s}{.}1$	$-70°51'27\overset{''}{.}1$	$16\overset{m}{.}00$	$-0\overset{m}{.}02$	$14\overset{m}{.}66$	$-0\overset{m}{.}36$	1.6	$+228$	0.0% (T304)
MJ8241	$01^h03^m25\overset{s}{.}0$	$-70°51'55\overset{''}{.}2$	$15\overset{m}{.}51$	$+0\overset{m}{.}12$	$15\overset{m}{.}74$	$+0\overset{m}{.}35$	2.4	$+244$	—
MJ8453	$01^h02^m00\overset{s}{.}1$	$-70°51'15\overset{''}{.}0$	$16\overset{m}{.}92$	$-0\overset{m}{.}15$	$15\overset{m}{.}90$	$-2\overset{m}{.}17$	4.0	$+73$	0.0% (T396)

$v_{rad,SMC} = +149$ km s^{-1} (Hatzidimitriou et al. 1997)
$v_{rad,47Tuc} = -19$ km s^{-1} (Pryor & Meylan 1993)
$v_{rad,NGC362} = +223$ km s^{-1} (Pryor & Meylan 1993)

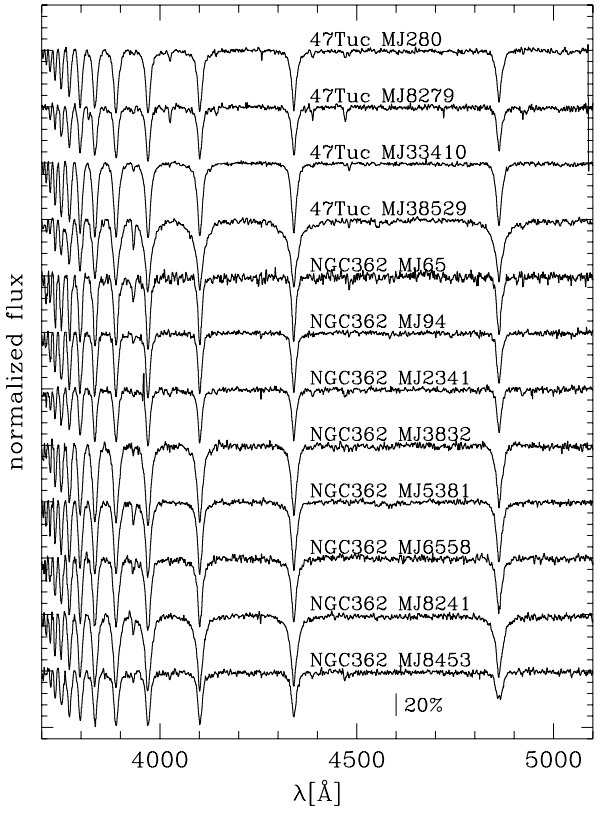

Fig. 2. The normalized medium resolution spectra of the target stars in 47 Tuc and NGC 362. The part shortward of 3900 Å was normalized by taking the highest flux point as continuum value.

were sometimes not close to the place of the object's spectrum. Nevertheless the flat field correction and wavelength calibration turned out to be good enough that a constant spatial distribution fit the sky light well enough to subtract the sky background at the object's position with sufficient accuracy. This means in our case that we do not see any absorption lines caused by the predominantly red stars of the clusters or by moon light. The fitted sky background was then subtracted from the unsmoothed frame and the spectra were extracted using Horne's algorithm (Horne 1986) as implemented in MIDAS.

Finally the spectra were corrected for atmospheric extinction using the data of Tüg (1977). The data for the flux standard stars were taken from Hamuy et al. (1992). The response curves were fitted by 8^{th} order polynomials for the low and medium resolution spectra. We took special care to correctly fit the response curves for the low resolution data in the region of the Balmer jump, since we planned to use this feature for the determination of the effective temperatures of the stars. The response curves showed a roughly constant shape, but varied in intensity, indicating non-photometric conditions during the observations.

We also used the medium resolution data to derive radial velocities, which are listed in Table 1 (corrected to heliocentric system). The error of the velocities is about 30 km s^{-1} (estimated from the r.m.s. scatter of the velocities derived from individual lines). The normalized and velocity-corrected spectra are plotted in Fig. 2.

4. Atmospheric parameters

4.1. $T_{\rm eff}$ *derived from energy distributions*

To avoid any spurious results due to contamination from neighbouring stars we searched all stars for red neighbours. For this purpose we used the photometry of 47 Tuc and NGC 362 (Montgomery & Janes, priv. comm.), and extracted for each of our targets all stars within a radius of 20″ (down to the limiting magnitude of $B \approx 18\overset{\rm m}{.}5$). We then estimated the straylight provided by these stars assuming that the seeing at larger distances is best described by a Lorentz profile and scaling the intensities with the V fluxes. We used 1″.5 as "intrinsic seeing" for all observations (which overestimates the seeing near the meridian) and took into account the elongation caused by atmospheric dispersion. Under these assumptions we get stray light levels of more than 3% in B only for *MJ3832* (36%) in NGC 362.

We used line blanketed LTE model atmospheres of Kurucz (1992, ATLAS9) for a metallicity [M/H] = −1.0 to derive effective temperatures from the low resolution spectra. To correct for interstellar reddening we applied the reddening law of Savage & Mathis (1979) and used an E_{B-V} of $0\overset{\rm m}{.}04$ for both clusters.

The simultaneous fitting of the spectrophotometric data (Balmer jump and continuum) was generally possible except for *MJ38529* in 47 Tuc and *MJ6558* and *MJ3832* in NGC 362. *MJ3832* has a cool star close by (*MJ3749*, distance 3″, B = $14\overset{\rm m}{.}39$, $B-V = +1\overset{\rm m}{.}43$) which contaminates the low resolution spectrum that was observed with a 5″ slit (see above). *MJ6558* was observed at rather high airmass (1.8) and *MJ38529* is probably a binary (see below). However, comparing our measured intensities to those derived from B and V magnitudes of the stars led to discrepancies of up to $0\overset{\rm m}{.}3$. In most of the cases the observed spectra were brighter than the corresponding photometric fluxes. The slope as derived from $B-V$ was consistent with the slope of the spectrophotometric continuum in most cases except *MJ38529* in 47 Tuc and *MJ5381* in NGC 362 ($B-V$ being more positive than indicated by the spectrophotometric continuum). These variations are consistent with non-photometric weather conditions, assuming that the varying atmospheric absorption was basically grey, i.e. independent of wavelength. If the absorption towards the flux standard stars were greater than towards the globular clusters, the cluster stars would be calibrated too bright. We found that the observed H_β line in the low resolution spectrum of *MJ8453* in NGC 362 was significantly shallower than the theoretical one (see also below).

4.2. Balmer line profile fits

To derive effective temperatures, surface gravities, and helium abundances we fitted the observed Balmer and helium lines with appropriate stellar model atmospheres. Beforehand we corrected the spectra for radial velocity shifts, derived from the positions of the Balmer lines. To establish the best fit we used the routines developed by Bergeron et al. (1992) and Saffer et al. (1994), which employ a χ^2 test. The σ necessary for the calculation of χ^2 is estimated from the noise in the continuum regions of the spectra. The fit program normalizes model spectra *and* observed spectra using the same points for the continuum definition. We computed model atmospheres using ATLAS9 (Kurucz 1991, priv. comm.) and used Lemke's version[1] of the LINFOR program (developed originally by Holweger, Steffen, and Steenbock at Kiel university) to compute a grid of theoretical spectra, which include the Balmer lines H_α to H_{22} and He I lines. The grid covered the ranges 8000 K$\leq T_{\rm eff} \leq$20,000 K, $2.5 \leq \log g \leq 6.0$, and −2.0, −1.0 in $\log \frac{n_{He}}{n_H}$ at metallicities of −1 and −0.75.

We fitted the Balmer lines from H_β to H_{12} (excluding H_ϵ because of the Ca II H line) and the He I lines $\lambda\lambda$ 4026 Å, 4388 Å, 4472 Å, 4713 Å, and 4922 Å (for $T_{\rm eff} \geq$ 10,500 K). For cooler stars we fitted only the Balmer lines for a fixed helium abundance of $\log \frac{n_{He}}{n_H} = -1$ (the helium abundance in these cooler stars should be close to solar as they should not be affected by diffusion). In the medium resolution spectrum of *MJ8453* the observed H_β line is significantly less deep than the theoretical one and also H_γ shows some evidence for filling. We therefore excluded those two lines from the fit for this star. Several stars above 10,500 K do not show He I lines. We nevertheless fitted those regions of the spectra, where the He I lines are expected, to obtain an upper limit of the He abundance.

To check for any effects of metallicity on the final results we fitted the spectra with models of [M/H] = −1.00 and [M/H] = −0.75. We found that in all cases except *MJ3832* in NGC 362 the differences in effective temperature and surface gravity were below 1% resp. 0.05 dex (2% and 0.11 dex for *MJ3832*). As the differences are below our expected errors we decided to use only the results for [M/H] = −1 for the further discussion, which lies between the metallicity for 47 Tuc ([M/H] = −0.71) and that of NGC 362 ([M/H] = −1.16).

The fit program gives r.m.s. errors derived from $\Delta\chi^2 = 2.71$ ($T_{\rm eff}$, $\log g$) resp. 3.53 ($T_{\rm eff}$, $\log g$, $\log \frac{n_{He}}{n_H}$). However, if χ^2 is not close to 1 (see Table 2) these errors will most likely underestimate the true errors. As the errors causing $\chi^2 > 1$ are most probably systematic (see below) they are hard to quantify. We decided to get an estimate of their size by assuming that the large χ^2 is solely caused by noise. Increasing the noise parameter σ until χ^2 = 1 then yields new formal errors for $\Delta\chi^2$ = 2.71 and 3.53, respectively, which are given in Table 2. These errors still underestimate the internal errors as we oversampled the spectra by a factor of 2.5 when rebinning to constant wavelength steps. Thus only 40% of the wavelength points used for the fit are truly independent. We correct this by applying a factor of $\sqrt{2.5} = 1.6$ to all error estimates. We believe that the χ^2 values above 1 are due to the low resolution of the data (5.7 Å): At $T_{\rm eff}$ = 11,000 K and $\log g$ = 4 the FWHM of the theoretical Balmer lines are around 12 Å. Thus the instrumental profile makes up a considerable part of the observed line profile. Therefore any deviations of the instrumental profile from a Gaussian (which is used to convolve the model spectra) will lead to a bad fit. Fortunately we could compare the effects for one hot HB star (B 3253) in NGC 6752, for which we have an NTT spectrum

[1] For a description see
http://a400.sternwarte.uni-erlangen.de/∼ai26/linfit/linfor.html

Table 2. Atmospheric parameters and masses for the programme stars as derived from low and medium resolution spectroscopic data. The surface gravities derived from the low resolution spectrophotometric data are rather uncertain. We also give the reduced χ^2 values from the line profile fits and the errors listed below are the r.m.s. errors of the fit routine adjusted as described in the text. The three rightmost columns give the cluster resp. SMC membership according to the radial velocity, proper motion, and derived mass of the star (see Sect. 5 for details). A — means that the information places a star neither to the globular cluster nor to the SMC. Brackets note dubious assignments.

Star	spectrophotometry			medium resolution data			Masses		membership		
	$T_{\rm eff}$ [K]	log g [cm/s^2]	χ^2	$T_{\rm eff}$ [K]	log g [cm/s^2]	log $\frac{n_{He}}{n_H}$	cluster [$M_\odot$]	SMC [$M_\odot$]	$v_{\rm rad}$	proper motion	mass
					47Tuc						
MJ280	13500	4.0:	2.75	14500±290	4.21±0.08	−1.41±0.16	0.65	133	C	C	C
MJ8279	18000	4.5:	1.96	18500±530	4.20±0.10	−1.56±0.11	0.02	3.8	SMC		SMC
MJ33410	10000	3.5:	4.53	10400±210	3.53±0.11	−1.00	0.51	104	C		C
MJ38529	8000[1]	3.0:	2.25	7950±20	5.21±0.05	−1.00	24	4900	C	C	—
	12500[2]	3.5:	7.85	14000±400	5.34±0.11	<−2	8.4	1700	C	C	—
					NGC362						
MJ65	8500	2.5:	2.03	9460±540	2.46±0.32	−1.00	0.16	9.5	SMC	—	SMC
MJ94	11000	3.5:	3.53	11700±350	3.33±0.11	−1.93±0.35	0.13	7.6	SMC	—	SMC
MJ2341	16000	4.5:	2.08	17400±500	3.97±0.10	−1.79±0.13	0.10	5.9	—		SMC
MJ3832			2.64	8250±140	2.77±0.06	−1.00	0.23	13	C		(C)
MJ5381	9000	3.0:	2.43	7780±100	2.14±0.05	−1.00	0.03	2.0	(SMC)	—	—
MJ6558			3.06	12500±350	4.09±0.11	−1.61±0.40	1.08	62	C	—	(C)
MJ8241	8500	3.5:	3.49	7980±50	3.06±0.06	−1.00	0.51	29	C		C
MJ8453[3]	14000	4.0:	1.53	16600±560	4.11±0.11	−1.99±0.11	0.27	18	—	—	(C)

[1] fitting the continuum
[2] fitting the Balmer jump
[3] H_β, H_γ are not included in the fit of *MJ8453*

with the same setup as is used here and a spectrum from the ESO 1.52m telescope with a resolution of 2.6 Å. While the reduced χ^2 values for the two spectra differ by a factor of 2 (5.9 vs. 3.1) the resulting effective temperatures and surface gravities are rather similar (13,700 K/3.75 vs. 13,700 K/3.80, see Moehler et al. 2000 for details).

4.3. Comparison of effective temperatures obtained with different methods

As can be seen from Table 2 the temperatures determined from the spectrophotometric data deviate from those derived from the Balmer lines, which may be an effect of strongly varying atmospheric extinction (as is already suggested by the discrepancies between spectrophotometric and photometric fluxes for the stars, see Sect. 4.1). Differences in the reddening and interstellar extinction law between galactic globular clusters and the SMC may also affect the flux distribution of the stars, which are by default only corrected for the galactic extinction towards the respective cluster. Sasselov et al. (1997) report that the extinction law for the SMC is essentially the same as that for the Large Magellanic Cloud (LMC). We therefore dereddened the extinction corrected spectra once more, this time using $E_{B-V} = 0^{\rm m}.09$ and the reddening law towards the LMC (Howarth 1983) as implemented in MIDAS. The resulting differences between spectra with and without this additional reddening correction

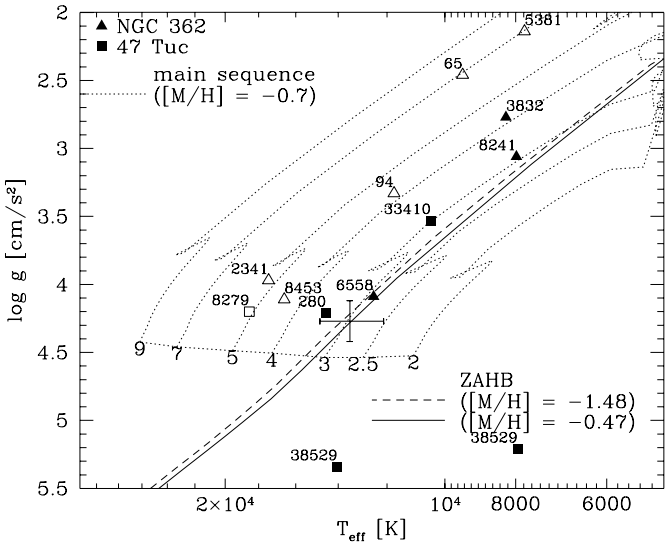

Fig. 3. The atmospheric parameters of the target stars in 47 Tuc and NGC 362 compared to zero-age horizontal branch models (Dorman et al. 1993, solid and dashed lines) and (post)-main-sequence models (Charbonnel et al. 1993, dotted lines). The numbers along the main sequence give the mass of the model star in solar masses. The suspected field/SMC stars are marked by open symbols.

are too small to explain the temperature differences between the results from the low resolution data and the line profiles. We

thus conclude that the most probable explanation for the discrepancies lies with the non-photometric observing conditions.

4.4. Masses

Knowing $T_{\rm eff}$, $\log g$, and the distances of the stars we can derive the masses:
$\log \frac{M}{M_\odot} = const. + \log g + 0.4 \cdot ((m-M)_V - V + V_{th})$
(V_{th} denotes the theoretical brightness at the stellar surface as given by Kurucz 1992.) The results are listed in Table 2. We determine two masses for each star, one assuming that it is a cluster member and one assuming it belongs to the SMC. We use the following reddening-free distance moduli $(m-M)_0$: $13\overset{\rm m}{.}31$ for 47 Tuc, $14\overset{\rm m}{.}67$ for NGC 362 (both from Djorgovski 1993; Harris 1996 gives $13\overset{\rm m}{.}25$ resp. $14\overset{\rm m}{.}65$ in the June 22, 1999 version of his compilation), and $18\overset{\rm m}{.}91$ for the SMC (Sasselov et al. 1997). Using the HIPPARCOS based distance moduli to 47 Tuc and NGC 362 of $13\overset{\rm m}{.}51$ and $14\overset{\rm m}{.}88$ (Gratton et al. 1997, Reid 1998) would increase the masses by about 20% in both cases.

In addition to the error in $\log g$ given in Table 2 errors in the absolute magnitude and the theoretical brightness at the stellar surface also enter the final error in $\log M$. We assume an uncertainty in the absolute brightness (combining errors in the photometric data, uncertainties in the distance moduli and reddenings) of $0\overset{\rm m}{.}3$, and a mean error in $\log g$ of 0.2 dex. The error in the theoretical V brightness is dominated by the errors in $T_{\rm eff}$. We estimate the total error in $\log M$ to be about 0.24 dex, corresponding to an error of $^{+73\%}_{-42\%}$ in mass (for a detailed discussion of error sources see Moehler et al. 1997).

5. Discussion

47 Tuc: As can be seen from Table 2 three of the four stars in 47 Tuc are probably members of the cluster, but *MJ8279* according to its radial velocity belongs to the SMC. The comparison of the spectroscopically derived mass ($3.8\,M_\odot$) with the mass obtained from the evolutionary tracks ($5\,M_\odot$) further supports its SMC membership. Kaluzny et al. (1997, 1998b) reported observations of six stars in the field of 47 Tuc with similar magnitudes and colors to *MJ 8279*, that is $18 < V < 18.7$, and $B-V \approx -0.1$. The evidence of *MJ 8279* supports their conclusion (based on a lack of a radial gradient) that most of these stars are probably SMC members.

Of the remaining three stars *MJ38529* is very probably a binary: Its UV-visual colour suggests an effective temperature of 11,900 K, but $B-V$ for this star is much too red[2] for such a temperature (see also its position in Fig. 1 below the HB). The optical low resolution spectrum suggests effective temperatures of 12,500 K (Balmer jump only) resp. 8000 K (continuum only). The superposition of two different stellar spectra (with different Balmer lines) may explain the strange values obtained for $\log g$ from the Balmer line profiles. If we assume that the temperature obtained from UV data is that of the hot component *MJ38529hot*, it would lie between *MJ280* and *MJ33410* in $T_{\rm eff}$. If *MJ38529hot* were a ZAHB star, its V magnitude should also lie between those two stars – in contradiction to the fact that the complete binary system is already fainter in V than *MJ280* and *MJ33410*. *MJ38529hot* could thus also be an extreme blue straggler, which would be fainter than a ZAHB star of the same $T_{\rm eff}$. On the other hand, the UV-based temperature is a lower limit for the hot component, as optical data are also involved in its determination (UV-visual colour). If *MJ38529hot* were considerably hotter than *MJ280* it would be much fainter visually and could therefore be a hot ZAHB star accompanied by a red subgiant. Thus the contamination by the cool star prevents any definite conclusions.

MJ280 is hot enough to be affected by diffusion processes which may result in an enrichment of heavy elements in its atmosphere (cf. Moehler et al. 2000). Fitting it with enriched model atmospheres as described by Moehler et al. (2000, [Fe/H] = +0.5) indeed yields $T_{\rm eff}$ = 14,200 K, $\log g$ = 4.29 and $\log \frac{n_{He}}{n_H}$ = −1.63, moving the star closer to the ZAHB.

MJ33410 finally is a normal cool HBB star. The masses of *MJ280* and *MJ33410* agree well with canonical predictions.

NGC 362: According to Table 1 three of the eight targets in NGC 362 are radial velocity members. *MJ6558* is not a proper motion member, but the error of its proper motion is rather large compared to the measurements of the other stars. *MJ6558* and *MJ8241* lie close to the canonical ZAHB, whereas *MJ3832* has evolved towards lower $\log g$. The mean mass of all three stars is $0.50^{+0.44}_{-0.23}\,M_\odot$ (r.m.s. errors only) and thus also in good agreement with canonical HB theory. Note that MJ6558 was one of the three candidate blue HB stars (= H1382) in NGC 362 identified by Harris (1982); the other two Harris candidates were not detected with UIT and radial velocity studies indicate that they are unlikely to be cluster members (R. Rood, priv. comm.). None of the radial velocity members are good candidates for being extreme blue stragglers, in the sense of having both a mass and $T_{\rm eff}$ consistent with being on an extension of the NGC 362 main sequence.

The three radial velocity member stars are all located within $2\farcm5$ of the cluster center, while the remaining five stars are all more than $3\farcm5$ from the center. Three of these five stars may belong to the SMC according to their radial velocities: *MJ65*, *MJ94*, and *MJ5381*. They lie, however, farther from the SMC main sequence in Fig. 1 than the remaining two stars *MJ2341* and *MJ8453*. Comparing the spectroscopically determined masses to those derived from evolutionary sequences would put *MJ65* ($9.5\,M_\odot$ vs. $7\,M_\odot$), *MJ94* ($7.6\,M_\odot$ vs. $4\,M_\odot$), and *MJ2341* ($5.9\,M_\odot$ vs. $5\,M_\odot$) to the SMC. The radial velocity of *MJ2341* differs by 74 km s^{-1} from that of the SMC, and so it might be a high-velocity halo star of the SMC (see, e.g., Keenan 1992, 1997 for a discussion of main-sequence B stars in the halos of galaxies). While two of the three stars lie away from the main sequence one should keep in mind that our selection is heavily biased towards bright (= evolved) hot SMC stars. Note that *MJ65* and *MJ94* appear to be normal HB stars in the UV CMD of Dorman et al. (1997), which emphasizes the need for

[2] Kaluzny et al. (1998a) give a relatively red $V-I$ colour of $\approx +0.14$ for *MJ38529*, which provides further evidence for the presence of a cool companion.

spectroscopic observations to verify the evolutionary status of stars in fields with high contamination.

The evolutionary status of *MJ5381* is unclear: In the $m_{162}, m_{162} - V$ diagram of Dorman et al. (1997) it lies rather isolated – being fainter than the theoretical ZAHB for NGC 362, but much cooler than the SMC main sequence.

The filled H_β line of *MJ8453* reminds us of the Be stars analysed by Mazzali et al. (1996), but it is considerably cooler than those objects. A spectrum of the H_α region of this star would be helpful to decide whether it indeed shows a Be-like spectrum.

6. Conclusions

There has been increasing interest in understanding the origin of the hot stars that can appear in old, metal-rich systems. The metal-rich open clusters NGC 6791 ([Fe/H] = +0.4) and NGC 188 ([Fe/H] = 0.0) contain hot HB populations sufficiently large that the UV-turnup in their integrated cluster spectra would be as strong as that observed in elliptical galaxies (Landsman et al. 1998). At these high metallicities, hot HB stars can be a natural product of single-star HB models (e.g. Dorman et al. 1993), although a significant fraction of the hot stars in the two clusters are binaries (Green et al. 1997). The metal-rich bulge globular clusters, NGC 6388 ([Fe/H] = -0.60, Harris 1996) and NGC 6441 ([Fe/H] = -0.53, Harris 1996) contain a sizable population of blue HB stars. A possible scenario for the blue HB in these clusters is a merger of two systems with different ages, with the blue HB arising from the minority old population (Yoon et al. 2000). However, this scenario does not explain several other peculiar aspects of the blue HB population in NGC 6388 and NGC 6441, including the slope of the HB, and the gravities which are higher than predicted by canonical models (Moehler et al. 1999).

Here we have shown that at least some hot HB stars exist in the classical red HB clusters 47 Tuc and NGC 362, and – unlike the case of NGC 6388 and NGC 6441 – they perfectly fit the expectations of canonical HB evolution. The three blue members in 47 Tuc all have 10,000 K $< T_{\rm eff} <$ 15,000 K, and thus are well separated from the rest of the HB population, which is (except for the single RR Lyr V9) entirely redward of the instability strip. (A fourth probable hot star member of 47 Tuc is UIT-14, which is only $1.7'$ from the cluster center, and for which the IUE spectrum obtained by O'Connell et al. 1997 indicates $T_{\rm eff} \approx$ 50,000 K.) The small number of hot HB stars in 47 Tuc, and their high temperatures, point to a scenario in which they have a different physical origin (such as binary interactions) than the dominant red HB population. It is suggestive that one of the hot stars in 47 Tuc (*MJ38529*) appears to be a photometric binary, whose hot component could, however, also be an extreme blue straggler.

Interestingly, whereas NGC 362 has 14 bright blue stars within $14''$ radius of its center (Dorman et al. 1997), the inner $1'$ of 47 Tuc probably does *not* contain any hot HB stars, as shown by observations with IUE (Rich et al. 1993), UIT (O'Connell et al. 1997), and WFPC2 (Rich et al. 1997). Rose & Deng (1999) found that only about 7% of the mid-UV light in the core of 47 Tuc comes from stars hotter than about 7,500 K (most of which are probably blue stragglers).

The three hot HB stars in NGC 362 are somewhat cooler than those in 47 Tuc, and the dominant HB in NGC 362 is not as red as that of 47 Tuc. Thus it is plausible that the blue HB stars in NGC 362 arise from a small percentage of red giants with unusually high mass loss, and no special mechanism is required for their production. Unfortunately, the SMC contamination is larger in NGC 362 than in 47 Tuc, and five out of our eight targets turned out to be nonmembers. It would be interesting to study the stellar parameters of the hot stars in the core region, which we could not observe due to high crowding, but where the relative SMC contamination should be much lower.

Acknowledgements. We want to thank the staff of the ESO La Silla observatory for their support during our observations and an anonymous referee for valuable comments. SM acknowledges support by the DLR (grant 50 OR 96029-ZA).

References

Bergeron P., Saffer R.A., Liebert J., 1992, ApJ 394, 228
Bailyn C., 1995, ARA&A 33, 133
Burgarella D., Paresce F., Meylan G., et al., 1994, A&A 287, 769
Carney B.W., Storm J., Williams C., 1993, PASP, 105,294
Catelan M., 2000, ApJ 531, 826
Charbonnel C., Meynet G., Maeder A., Schaller G., Schaerer D., 1993, A&AS 101, 415
Djorgovski S., 1993, In: Djorgovski S.. G. Meylan (eds.) ASP Conf. Ser. 50, Structure and Dynamics of Globular Clusters. ASP, San Francisco, p. 373
Dorman B., Rood R.T., O'Connell R.W., 1993, ApJ 419, 596
Dorman B., O'Connell R.W., Rood R.T., 1995, ApJ 442, 105
Dorman B., Shah R.Y., O'Connell R.W., et al., 1997, ApJ 480, L31
Ferraro F.R., Paltrinieri B., Fusi Pecci F., et al., 1997a, ApJ 484, L145
Ferraro F.R., Paltrinieri B., Fusi Pecci F., et al., 1997b, A&A 324, 915
Fusi Pecci F., Ferraro F.R., Bellazzini M., et al., 1993, AJ 105, 1144
Gardiner L.T., Hatzidimitriou D., 1992, MNRAS 257, 195
Gratton R.G., Fusi Pecci F., Carretta E., et al., 1997, ApJ 491, 749
Green E.M., Liebert J.W., Saffer R. 1997, In: Philip A.G.D., Liebert J., Saffer R.A. (eds.) The 3^{rd} Conf. on Faint Blue Stars. L. Davis Press, Schenectady, p. 417
Hamuy M., Walker A.R., Suntzeff N.B., et al., 1992, PASP 104, 533
Harris W.E., 1982, ApJS 50 573
Harris W.E., 1996, AJ 112, 1487
Hatzidimitriou D., Croke B.F., Morgan D.H., Cannon R.D., 1997, A&AS 122, 507
Horne K., 1986, PASP 98, 609
Howarth I.D., 1983, MNRAS 203, 301
Kaluzny J., Krzemisńki W., Mazur B., Wysocka A., Stepień K., 1997, Acta Astron. 47, 249
Kaluzny J., Kubiak M., Szymanski M., et al., 1998a, A&AS 128, 19
Kaluzny J., Wysocka A., Stanek K.Z., Krzemiński W., 1998b, Acta. Astron. 48, 439
Keenan F.P., 1992, QJRAS 33, 325
Keenan F.P., 1997, In: Philip A.G.D., Liebert J., Saffer R.A. (eds.) The 3^{rd} Conf. on Faint Blue Stars. L. Davis Press, Schenectady, p. 199
Kurucz R.L., 1992, In: Proc. IAU Symp. 149, The Stellar Populations of Galaxies. Kluwer, Dordrecht, p. 225

Landsman W., Bohlin R.C., Neff S.G., et al., 1998, ApJ 116, 789
Mazzali P.A., Lennon D.J., Pasian F., et al., 1996, A&A 316, 173
Moehler S., Heber U., Rupprecht G., 1997, A&A 319, 109
Moehler S., Sweigart A.V., Catelan M., 1999, A&A 351, 519
Moehler S., Sweigart A.V., Heber U., Landsman W.B., 2000, A&A 360, 120
O'Connell R.W., Dorman B., Shah R.Y., et al., 1997, AJ 114, 1982
Park J.-H., Lee Y.-W., 1997, ApJ 476, 28
Pryor C., Meylan G., 1993, In: Djorgovski S., Meylan G.(eds.) ASP Conf. Ser. 50, Structure and Dynamics of Globular Clusters. ASP, San Francisco, p. 357
Reid I.N., 1998, AJ 115, 204
Rich R.M., Minniti D., Liebert J., 1993, ApJ 406, 489
Rich R.M., Sosin C., Djorgovski S.G., et al., 1997, ApJ 484, L25
Rose J.A., Deng S., 1999, AJ 117, 2213
Saffer R.A., Bergeron P., Koester D., Liebert J., 1994, ApJ 432, 351
Sarajedini A., Lee Y.-W., Lee D.-H, 1995, ApJ 450, 712
Sasselov D.D., Beaulieu J.P., Renault C., et al., 1997, A&A 324, 471
Savage B.D., Mathis F.S., 1979, ARA&A 17, 73
Sepinsky J.F., Saffer R.A., Pilman C.S., DeMarchi G., Paresce F., 2000, BAAS 32, 740
Stetson P.B., VandenBerg D.A., Bolte M., 1996, PASP 108, 560
Tucholke H.-J., 1992a, A&AS 93, 293
Tucholke H.-J., 1992b, A&AS 93, 311
Tüg H., 1977, ESO Messenger 11, 7
Yoon S.-J., Lee C.-H., Lee Y.-W., 2000, BAAS 32, 739